ELSEVIER

Journal of Nuclear Materials 266–269 (1999) 766–770

journal of nuclear materials

Effect of the velocity shear on particle transport and edge turbulence in a reversed field pinch

V. Antoni [a,b,*], R. Cavazzana [a], E. Martines [a], G. Serianni [a], M. Bagatin [a,b], D. Desideri [a,b], M. Moresco [a,b], E. Spada [a], L. Tramontin [a]

[a] *Consorzio RFX, corso Stati Uniti 4, 35127 Padova, Italy*
[b] *INFM, Unità di Padova sez. A, Padova, Italy*

Abstract

In this paper the results of the investigation of the edge turbulence performed in RFX by a set of Langmuir probes and a homodyne reflectometer are reported. The electrostatic turbulence exhibits large fluctuation amplitude and broad band features in frequency and wavenumber. The effect of the spontaneous $\mathbf{E} \times \mathbf{B}$ velocity shear layer observed at the edge is addressed in order to identify decorrelation effects on the turbulence. Similarities with tokamaks and stellarators are discussed.

Keywords: Turbulence; RFX; Reversed field pinch; Fluctuation

1. Introduction

The role of electrostatic turbulence in the energy and particle transport in plasmas confined in reversed field pinch (RFP) configuration is an outstanding issue in the study of the anomalous transport in these experiments. This study is aimed at understanding the mechanism and obtaining transport reduction at the edge via boundary plasma control as performed in tokamaks and stellarators [1]. Electrostatic turbulence has been demonstrated to drive most of the particle transport at the edge as in tokamaks and stellarators. Recently, regimes of improved confinement have also been observed in RFPs and interpreted as being related to a change of the $\mathbf{E} \times \mathbf{B}$ velocity shear at the edge [2]. At the edge of RFX it has been found that a spontaneous double $\mathbf{E} \times \mathbf{B}$ velocity shear layer occurs [3] and that the shear value is close to that required for turbulence decorrelation [4]. This paper aims to characterize the edge turbulence in the experiment RFX ($R = 2$ m, $a = 0.457$ m) and to the study of the effect of the velocity shear on the fluctuation properties.

2. Experimental set-up

The data reported in this paper refer to an experimental campaign at low plasma current $I = 300$–400 kA. It is worthy to note that in the RFP configuration the magnetic field at the edge is mainly poloidal, so that the toroidal direction is mainly perpendicular to the magnetic field and the Larmor radius typically an order of magnitude larger than in tokamaks with comparable plasma current. The reversal of the toroidal magnetic field, which typically takes place at $r/a \sim 0.85$–0.9, identifies an outer region, where the toroidal field has a direction opposite to that in the core. It is worth noting that in this region, since the safety factor q crosses zero, the magnetic field shear is much higher than that in tokamaks and stellarators. The experimental equipment consists of Langmuir probes and a homodyne reflectometer. The probes are housed in a boron nitride head whose dimensions are 60 mm height and 100 mm width. The head is inserted through an equatorial port by a system which allows linear translation and rotation around the symmetry axis. The probe electrodes are graphite pins flush with the head surface, with a diameter of 2 mm. The head and the probes have been moved in between the shots to scan the edge region up to 60 mm insertion. The pin surface is oriented at 45° with respect

* Corresponding author. Tel.: +39-049 829 5033; fax: +39-049 870 0718; e-mail: antoni@igi.pd.cnr.it

0022-3115/99/$ – see front matter
PII: S0022-3115(98)00842-3

to the magnetic field. A diagram of the head and probes is shown in Fig. 1. The pins closer to the unperturbed plasma are located 2.2 mm right behind the head tip. The pins have been aligned in the toroidal direction so as to have the same poloidal positions. At the time of measurement of the data presented here, two floating potential measurements (V_f) and an ion saturation current (I_s) measurement were used to study the electrostatic fluctuation properties and the electrostatic radial particle flux. One of the two V_f measurements was obtained from two electrically connected pins located on either side of the pin measuring I_s, so that the V_f and I_s measurements can be considered to be taken at the same location (Fig. 1). The two V_f measurements were 44 mm toroidally apart. It is known that the finite perpendicular separation between the pins can induce a phase delay error equal to $\cos(2kd)$ [5] where d is the distance between the pins and k the perpendicular wave vector. In the present case d is 5 mm whereas k, as reported in the following, is typically in the range 10–30 m^{-1}, so that even in the worst case the relative phase error results less than 5%. The distance between the pins measuring the floating potential has been changed from 44 to 88 mm (using V_{fB} instead of V_{fC} of Fig. 1) in order to test the k resolution. In the latter configuration aliasing features occurred in the $S(k, f)$ spectra so that the former arrangement is preferable to resolve the smallest wavelengths (highest wavenumbers) which are present in the edge of RFX.

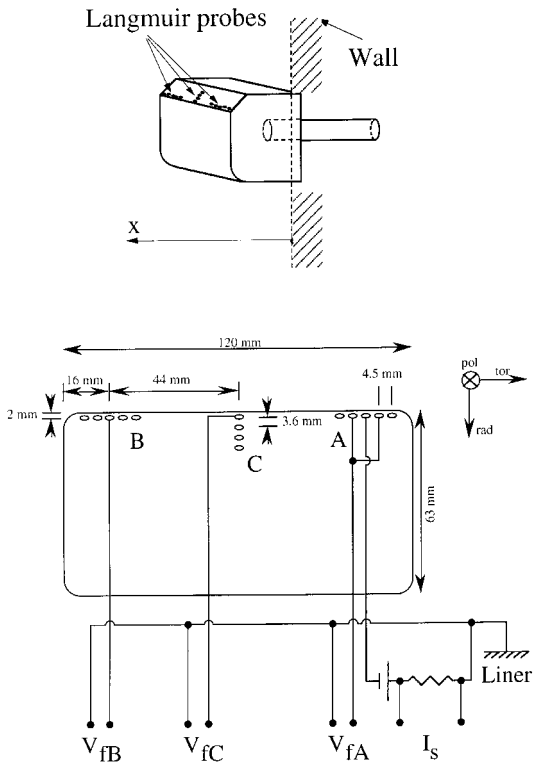

Fig. 1. Diagram of the head equipped with Langmuir probes and diagram of the electric connections.

Data have been transferred via fibre optic link to avoid ground loops and reduce noise pick-up. The fluctuation data have been measured with a bandwidth dc $< f <$ 500 kHz and have been analysed in the time and wavenumber–frequency domain. For the frequency analysis the signal has been divided into many (~100) time slices which have been treated as independent realisations. Only fluctuations during the RFP sustainment phase have been considered. All the measurements were made while keeping the probes on the head side protected with respect to the unidirectional superthermal electron flow which is found in the edge of RFP plasmas.

The microwave reflectometer operating on RFX is a frequency modulated continuous wave type with homodyne detection [6], upgraded to operate at ultrafast sweeps rate (up to 4 GHz/μs) in the K_a band [7]. At such high sweep rates, fringe jumps caused by density fluctuations are removed and the detected signal is clear enough to obtain separate phase and amplitude measurements. Plasma measurements were taken using two different modulation schemes, alternated every 250 μs during the same discharge. One scheme uses a frequency range between 34 and 38 GHz (critical electron densities: 1.4×10^{19}–1.8×10^{19} m^{-3}), swept in 1 μs with a repetition rate of 1.25 μs, in order to measure the electron density gradient and the reflected power level at different frequencies. The second scheme is aimed to obtain a more detailed time evolution of the phase and power signals by means of a shorter sweep of 250 ns in the range 35.5–36.5 GHz, corresponding to densities in the range 1.56×10^{19}–1.65×10^{19} m^{-3}. In both cases the reflectometric signal at the detector is sampled at 250 Msamples/s.

3. Results

As pointed out in the introduction, a double $\mathbf{E} \times \mathbf{B}$ velocity shear occurs in the edge region of RFX, extending, for the present range of plasma current, in the region $0.92 < r/a < 1.02$. In this region, the normalised root mean square amplitude of the fluctuation of the floating potential V_f and ion saturation current I_s are typically $e\delta V_f/T_e \sim 1.5$ and $\delta I_s/I_s \sim 0.5$–1. It has been already reported [2] that in all RFPs these fluctuations have an amplitude comparable to that measured in tokamaks and stellarators. The normalized amplitude at the edge is plotted in Fig. 2 as a function of the normalized radius. In the same figure the radial extent of the two velocity shear layers measured in the same set of discharges is shown. The relative amplitude of the I_s

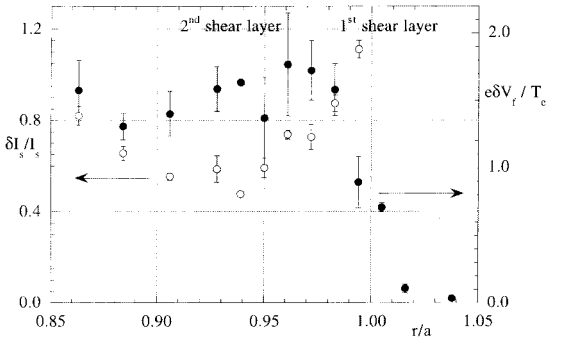

Fig. 2. Radial behaviour of normalised amplitude of floating potential and ion saturation current fluctuation. In the same figure the radial extension of the double velocity shear layer is also depicted. The radial position is normalized to the minor radius.

fluctuations, which mainly represent the density fluctuations, has a clear minimum in the middle of the second velocity shear layer, i.e. the more internal one, whereas the V_f fluctuations are slightly affected. V_f/T_e fluctuations decrease sharply in the first velocity layer close to the wall. This behaviour could be related to the presence of the wall as reported below for the diffusion coefficient which manifests the same behaviour. An example of spectral power density $S(k, f)$ [8] for V_f is shown in Fig. 3. As in tokamaks and stellarators the electrostatic turbulence exhibits broadband features as reported below. The spectrum displays on average a linear relationship between frequency and wavenumber, which gives a phase velocity of the order of 10^4 m/s and which can be mainly attributed to the Doppler effect caused by the $\mathbf{E} \times \mathbf{B}$ plasma rotation. The power spectrum of the reflectometric phase signal has a clear f^{-2} behaviour which does not depend on the underlying fluctuation structure, as expected when fluctuation levels are above a certain threshold [9]. On the other hand the power spectrum of the reflected microwave power has an identifiable structure. In Fig. 4 this spectrum and the spectrum of the ion saturation current of Langmuir probes are plotted for comparison. The two spectra are similar with the reflectometer signal spectrum shifted in frequency by a factor two. A similar behaviour has been reported in some cases comparing the phase signal spectrum with the reflected power signal spectrum [10]. In particular both spectra show a power law decay for $f > 100$ kHz, with a decay exponent equal to -2.5. A similar decay is found also on the V_f power spectrum. The average wavevector $\langle k \rangle$, defined as in [8], is equal to 10–20 m^{-1} as shown in Fig. 5. The spectral width σ_k [8], also shown in the same figure, is comparable to $\langle k \rangle$ so that the relative spectral broadening $\sigma_k/\langle k \rangle$ is almost unity independent of the velocity shear. The same relative broadening is found for the average frequency $\langle f \rangle$ and the relative spectral width σ_f. Fig. 5 shows that in the region of high velocity shear, in proximity of the point $r/a = 0.94$, $\langle k \rangle$ reaches a minimum. This can be interpreted as an indication that in this region a mechanism is acting which suppresses the highest wavenumbers. A similar behaviour is observed for the radial

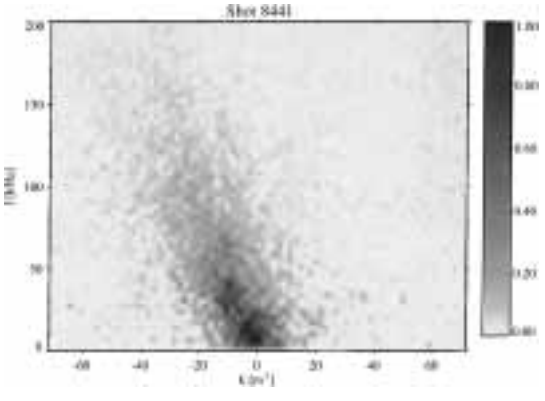

Fig. 3. Spectral power density $S(k, f)$ for floating potential fluctuations.

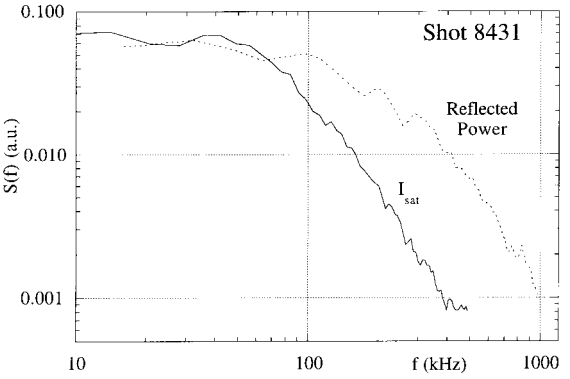

Fig. 4. Power spectrum of ion saturation current fluctuations and reflected power.

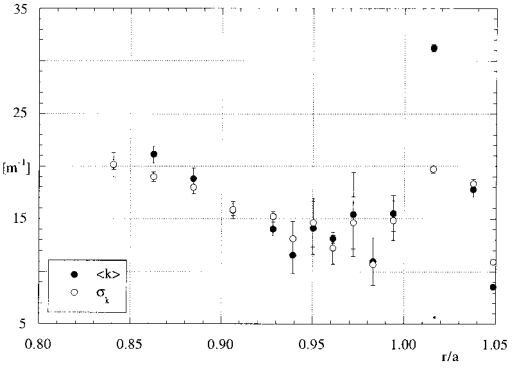

Fig. 5. Average k and spectral width σ_k vs r/a.

profile of the power weighted frequency, which has a minimum in the same region.

The range in k corresponds to a range in toroidal periodicity $20< n <40$ similar to that observed in other RFP experiments [2]. As in tokamaks and stellarators [1] the perpendicular wavelength is larger than the Larmor radius r_L, being typically $kr_L \sim 0.05$–0.1.

The radial correlation length has been measured by the reflectometer. It is known that in this fluctuation regime the measurement of the radial correlation length obtained from the phase signal gives wrong values [9]. However to get an estimate the radial correlation it is still possible to use the reflected power level [11].

To determine the radial correlation length, the cross correlation between couples of reflected microwave power signals $P_i(t)$ and $P_j(t)$, obtained at different probing frequencies f_i and f_j, is calculated as a function of the difference of probing frequencies $\Delta f = f_i - f_j$, to which corresponds a difference in density Δn:

$$C(\Delta n) = \frac{\langle P_{ni}(t) P_{nj}(t) \rangle}{\sqrt{\langle P_{ni}(t) \rangle^2 \langle P_{nj}(t) \rangle^2}} \approx \exp\left(-\frac{\Delta n}{N} \right)$$

The radial correlation length is calculated dividing the correlation density N by the density gradient in that region, $\Delta = N/(\mathrm{d}n/\mathrm{d}r)$. Finally since the sampling of power signals is not strictly simultaneous, a correction is made to take into account the introduced decorrelation [4].

The radial correlation length Δ measurement obtained by the reflectometer in the middle of the second velocity shear layer, at $r/a = 0.94$ results in $\Delta = 12$ mm, with a standard deviation of 5 mm. The characteristic density scale length, defined as $L_n = n/\nabla n$, with the density gradient $\nabla n = 6 \times 10^{20}$ m^{-4} almost constant in the edge region, varies, in the region $0.86< r/a <1$ from 60–10 mm. Thus comparing with the local $L_n \sim 20$ mm at $r/a \sim 0.94$, Δ is shorter than L_n.

The results reported above indicate that the velocity shear seems to affect some of the properties of the electrostatic fluctuations. As pointed out in Ref. [4], the velocity shear layer is, within the error bars, close to the condition required for the BDT decorrelation mechanism to apply on the electrostatic turbulence [12]. Indeed the shearing frequency ω_s, which can be estimated as $\omega_s = \langle k \rangle \Delta \, \mathrm{d}v_{\mathbf{E}\times\mathbf{B}}/\mathrm{d}r$, where $\mathrm{d}v_{\mathbf{E}\times\mathbf{B}}/\mathrm{d}r$ is the radial derivative of the $\mathbf{E}\times\mathbf{B}$ velocity, in the region of high velocity shear ($r/a = 0.94$), results $\omega_s = (1.6 \pm 0.9) \times 10^5$ rad/s, i.e. close to the ambient turbulence $\Delta\omega_t = (3.3 \pm 0.3) \times 10^5$ rad/s. The ω_s value has been derived from the experimental data of the quantities entering in the definition: $\mathrm{d}v_{\mathbf{E}\times\mathbf{B}}/\mathrm{d}r = (1.1 \pm 0.4) \times 10^6$ s^{-1}, $\langle k \rangle = 12 \pm 2$ m^{-1} and $\Delta = 12 \pm 5$ mm.

It has been reported [4] that the perpendicular particle flux driven by electrostatic fluctuations Γ_{es}, computed neglecting the temperature fluctuations, is comparable to the total particle flux. This result, common to other RFPs, constitutes, together with the observed velocity shear layer at the edge, one of the most remarkable similarities with tokamaks and stellarators. In Fig. 6 the frequency resolved particle flux $\Gamma(\omega)$, obtained at $r/a = 0.96$ where it is maximum, is shown. Particle transport peaks close to 100 kHz, and is mostly concentrated below 300 kHz. The coherence between the signals entering in the flux estimate, V_f and I_s, is high, with values ranging from 0.4 to 0.6 over the whole explored frequency range, and decreases in the more internal velocity shear layer, whereas their average relative phase, almost independent of frequency, does not. It has been found that the particle flux has a maximum at $r/a = 0.97$ and decreases in correspondence to the more internal velocity shear layer [4]. An effective perpendicular diffusion coefficient D_{es} has been derived assuming a Fick's diffusion law, i.e. $\Gamma_{es} = -D_{es}\nabla n$ with the constant density gradient reported above. The resulting diffusion coefficient is plotted in Fig. 7. Following the Γ_{es} be-

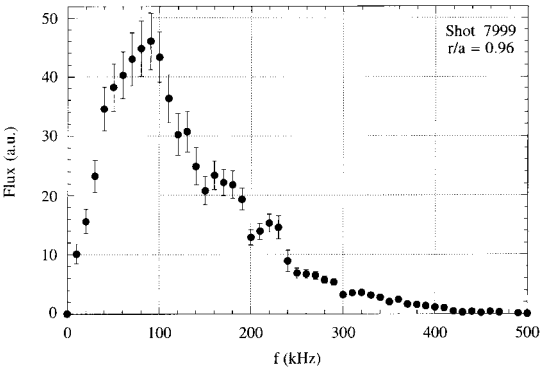

Fig. 6. Power spectrum of the particle flux.

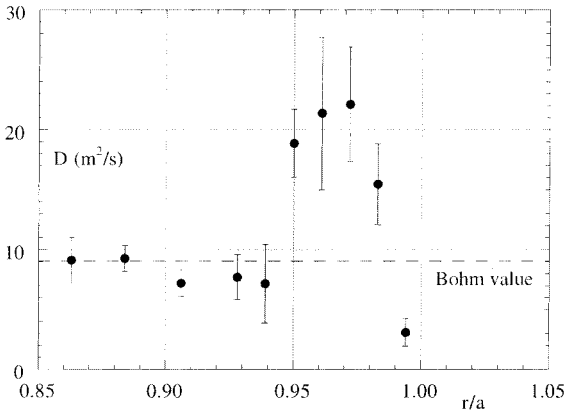

Fig. 7. Effective diffusion coefficient and Bohm estimate vs r/a. On the same figure the radial extension of the double velocity shear layer is also shown.

haviour, it decreases in the second velocity shear layer region to a value which is almost half of the maximum at $r/a \sim 0.97$, where the shear vanishes. The decrease of D_{es} towards the wall tracks the reduction observed for Γ_{es} and is a common feature of other devices [13]. This has been interpreted as due to parallel losses to the wall, an effect which is expected to be even more important in RFPs because of the larger magnetic fluctuations. For comparison, in the same figure, the Bohm diffusion coefficient estimated with the experimental edge electron temperature is also shown. The two estimates are consistent within a factor two. A more detailed study of the edge diffusivity is reported in Ref. [14] where the diffusion coefficient derived from local particle balance is compared with the effective value from electrostatic turbulence.

4. Discussion and conclusions

Edge turbulence at the edge of RFX shares many remarkable similarities with turbulence in tokamaks and stellarators such as broad band features and large normalised amplitude.

The velocity shear seems to affect the particle transport, which is mainly driven by these fluctuations, and then the diffusion coefficient, by decreasing the fluctuation average wavenumber and frequency, the ion saturation current normalized amplitude and the coherence between ion saturation current and floating potential.

Methods based on polarised electrodes are under investigation to modify the radial electric field at the edge to study and possibly further enhance these effects on the electrostatic turbulence.

References

[1] B.A. Carreras, IEEE Trans. Plasma Sci. 25 (1997) 1281.
[2] V. Antoni, Plasma Phys. Control. Fusion 39 (1997) B223.
[3] V. Antoni et al., Phys. Rev. Lett. 79 (1997) 4814.
[4] V. Antoni et al., Phys. Rev. Lett. 80 (1998) 4185.
[5] H.Y.W. Tsui et al., Rev. Sci. Instrum. 63 (1992) 4610.
[6] M. Moresco et al., Int. J. Infrared mm Waves, 12 (1992) 609.
[7] R. Cavazzana et al., 24th EPS Conf., Vol. 21C (1997) 361.
[8] S.J. Levinson et al. Nucl. Fusion 24 (1984) 527.
[9] E. Mazzucato, R. Nazikian, Rev. Sci. Instrum. 66 (1995) 392.
[10] G.D. Conway, 2D Physical Optics Simulation of Fluct Reflectometry, JET-P(97) 14.
[11] G.D. Conway, Plasma Phys. Control. Fusion 39 (1997) 407.
[12] H. Biglari, P.H. Diamond, P.W. Terry, Phys. Fluids B 2 (1990) 1.
[13] H.Y.W. Tsui et al., Phys. Fluids B 5 (1993) 2491.
[14] M. Bagatin et al, these Proceedings.